CNRS
Centre National de la Recherche Scientifique

INFN
Instituto Nazionale di Fisica Nucleare

Advanced Virgo SDB2 B1/B1p timing for O2

D. Estevez, V. Germain, F. Marion, A. Masserot, B. Mours, L. Rolland, D. Verkindt

VIR-0773A-17

October 16, 2017

VIRGO * A joint CNRS-INFN Project
Project office: Traversa H di via Macerata - I-56021 S. Stefano a Macerata, Cascina (PI)
Secretariat: Telephone (39) 50 752 521 – Fax (39) 50 752 550 – e-mail virgo@pisa.infn.it

Contents

Introduction

This note gives the timing of the detection bench SDB2_B1/B1p photodiode channels used for the O2 run. The SDB2_B1 bench is used for the reconstruction of the gravitational waves signal h_{rec} during the observations and SDB2_B1p is used for the calibration of the mirror actuators [1] [2]. The measurements were done a few days before the start of O2.
First, the measurements are given with both overall delay measurement, and intermediate measurements along the digital chain. Then the expected delays are given and compared to the measurements.

1 SDB2 B1/B1p timing measurements

1.1 Sensing path for B1/B1p timing

The set-up of the sensing chain for B1/B1p is shown in Figure 1.
The signal received by the photodiode is split in three channels allowing different ranges of frequencies :

- The DC channel results from a low-pass filtering of the raw signal.
- The Audio channel which keeps frequencies according to a band-pass filter.
- The RF channel for the high frequencies of the raw signal.

The two first signals are similarly processed and the RF signal is processed by a FPGA after a fast ADC. Here, we only describe the Audio path since it is the one we use for our measurements. After the photodiode and the pre-amplifer, the Audio signal is sent to a DAQ-Box to be filtered by an analog filter and converted into a digital signal sampled at 1 MHz by an ADC. Then the signal passes through a DSP processing a 8^{th} order Butterworth filter with $f_{cut} = 37518$ Hz and a decimation to generate a signal at 100 kHz. The DAQ-Box sends this signal to the RTPC by packets at 10 kHz. In the RTPC, the signal is sent to an ACL process processing a modified 8^{th} order Butterworth filter with $f_{cut} = 10$ kHz and a decimation process to eventually generate the output signal at 20 kHz.
The RTPC permanently delivers DC, Audio, Blended and 20 kHz channels, and also an Audio channel at 100 kHz delayed by one cycle of the ACL process without being filtered.

1.2 Measurements of the delays

In order to measure the delay of the sensing path, we use an IRIG-B signal provided by the GPS standard clock which is sent to a LED in front of the photodiodes SDB2_B1p_PD1 and SDB2_B1_PD2 with a delay we neglect (the signal propagates through a 21 m copper cable). The IRIG-B signal contains a pulse every second lasting 8 ms with a rising edge at the position

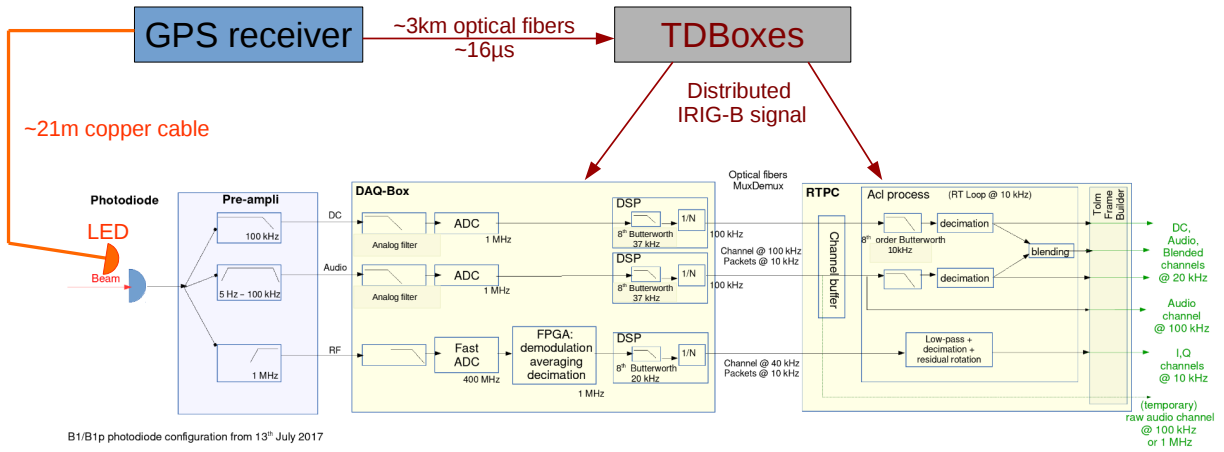

Figure 1: Sensing chain for SDB2_B1/B1p

of the start of the second. This signal is processed all along the sensing chain and one can access different output channels.
We report several measurements which were done by putting a LED receiving the IRIG-B signal in front of the photodiodes SDB2_B1p_PD1 and SDB2_B1_PD2 and looking at the signals after the different parts of the sensing path.

1.2.1 Audio 1 MHz channel after the ADC in the DAQ-Box

The 1 MHz signals after the first ADC for B1p_PD1 and B1_PD2 have been saved during ~ 30 s in the raw full files for dedicated measurements on the 26^{th} of July 2017.
Figure 2 represents a few microseconds of these channels around a rising edge of the IRIG-B signal seen by the photodiode. The rising edge has a minus sign on the Figure and we count the number of bins between the start and the second to get the delay of the signal. Since the signal is sampled at 1 MHz, one bin represents 1 μs. Here we evaluate a delay of $\tau_0 \sim -12 \pm 1$ μs for this channel. The minus sign for the delay indicates that the signal is actually in phase advance due to the 3 km optical fibers which distributes the IRIG-B signal to the DAQ-Box and counts for 16 ± 1 μs. Hence the delay of the analog part in the photodiodesensing is $\tau_{ana} = -12 + 16 = 4 \pm 2$ μs.

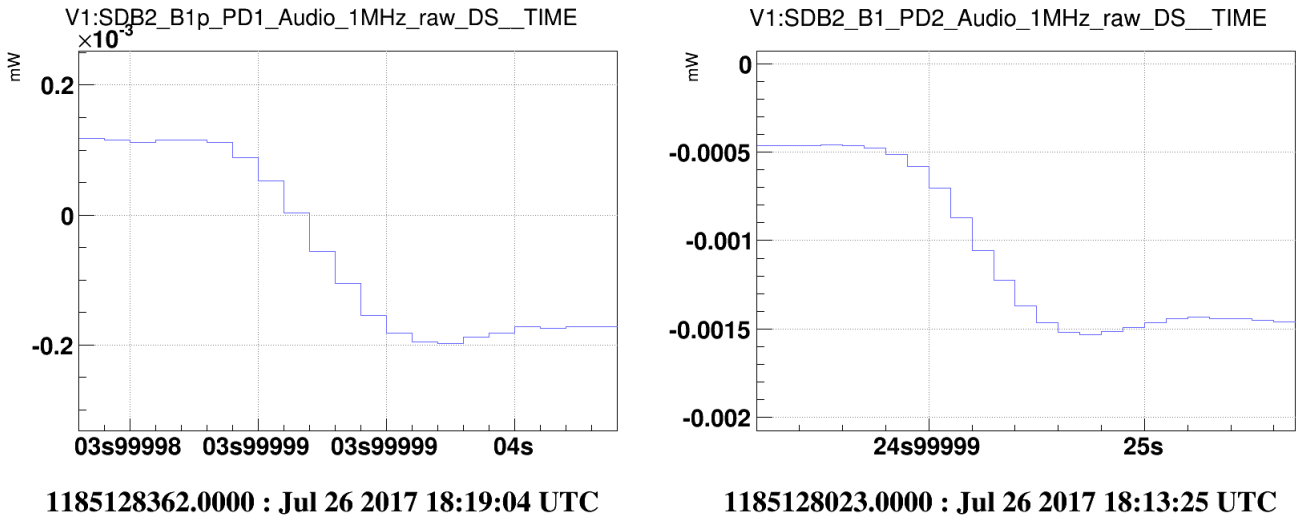

Figure 2: The 1 MHz signals for B1p_PD1 on the left and B1_PD2 on the right. Both delays are estimated at $\tau_0 = -12 \pm 1$ *µs.*

1.2.2 Audio 100 kHz channel after the DSP in the DAQ-Box

The 100 kHz signal after the DSP has only been saved[1] for B1_PD2 during $\sim$ 30 s in the raw full files for dedicated measurements on the 26^{th} of July 2017.
Figure 3a shows a delay between 100 μs and 120 μs where the size of the bins limits the accuracy on the delay to a step of 10 μs. In order to have a better accuracy we computed the transfer function between the 100 kHz channel and the previous 1 MHz channel to get the value of this delay inferred by the phase, see Figure 3b. Assuming the phase follows a linear delay, it can be expressed as: $\phi = -2\pi f\tau$ with f sweeping the frequency range and τ a delay. The phase has been fitted from 10 Hz to 2 kHz. The fit result and residuals are shown in Figure 3c. The fit of the delay is $\tau_{100kHz/1MHz} \sim 112.8 \pm 0.1$ μs with negligible statistical errors. The residuals enable to estimate the systematic uncertainty to be of the order of 1 mrad, corresponding to 0.1 μs at 2 kHz.

1.2.3 Audio 20 kHz channel at the output of the RTPC

The output signal of the RTPC at 20 kHz has a delay between 150 μs and 200 μs as we can see in Figures 4a, 4b. We can evaluate the transfer function between the 20 kHz channel and the 1 MHz channel to obtain the delay between these two channels using the phase, see Figure 4c. The delays corresponding to these phases are $\tau_{B1p} = \tau_{B1} = 151.9 \pm 0.2$ μs $= \tau_{20kHz/1MHz}$ as we can see on Figures 5a, 5b. For reasons of consistency and to understand well each step of the sensing path, we also evaluate the transfer function between the 20 kHz signal and the

[1] the files are stored in /data/procdata/calibration/rawdataCalibration/SDB2timing

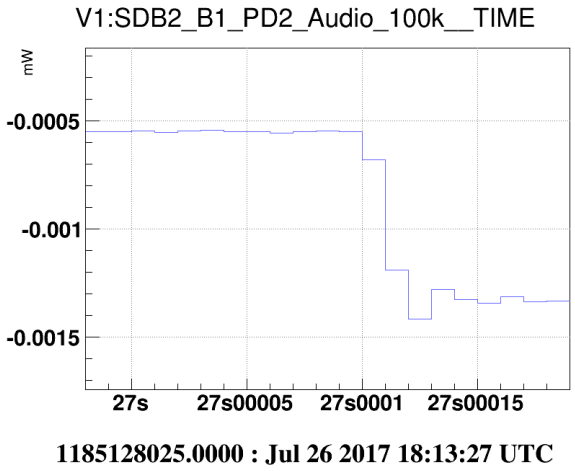

(a) The audio channel at 100 *kHz after the ADC. The delay is estimated at* $100\ \mu s \leq \tau_{100kHz/1MHz} \leq 120\ \mu s$.

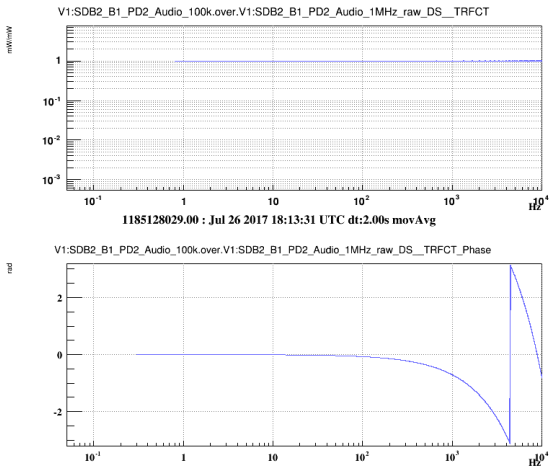

(b) The audio channel at 100 *kHz after the ADC. The delay is estimated at* $100\ \mu s \leq \tau_{100kHz/1MHz} \leq 120\ \mu s$.

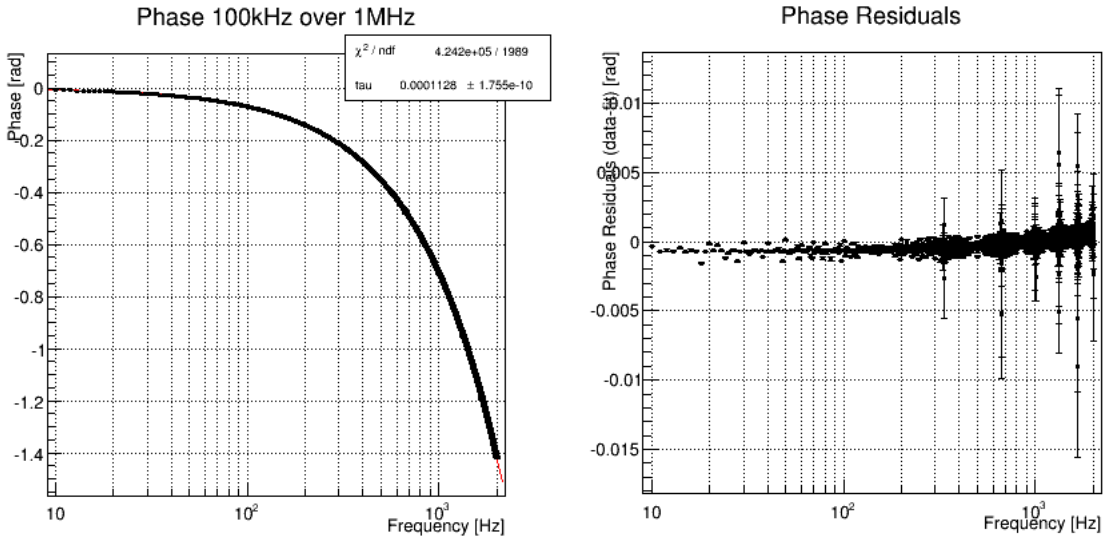

(c) Fit of the phase between the 100 *kHz channel and the* 1 *MHz channel (left panel) and the residuals (right panel). The delay is fitted at* $\tau_{100kHz/1MHz} \sim 112.8\ \mu s$ *with systematic uncertainty* $\leq 0.1\ \mu s$.

Figure 3: Audio signal at 100 kHz after the DSP, and transfer function between 100 kHz and 1 MHz.

100 kHz channel for B1_PD2, see Figure 6a. The phase can be approximated with a delay $\tau_{20kHz/100kHz} = 39.2 \pm 0.2\ \mu$s accounting for small deviations from a pure delay (Figure 6b). This value of the delay is consistent with the one expected regarding the other transfer functions previously computed. $\tau_{20kHz/1MHz} - \tau_{100kHz/1MHz} = 151.9 - 112.8 = 39.1 \pm 0.3\ \mu$s $\sim \tau_{20kHz/100kHz}$

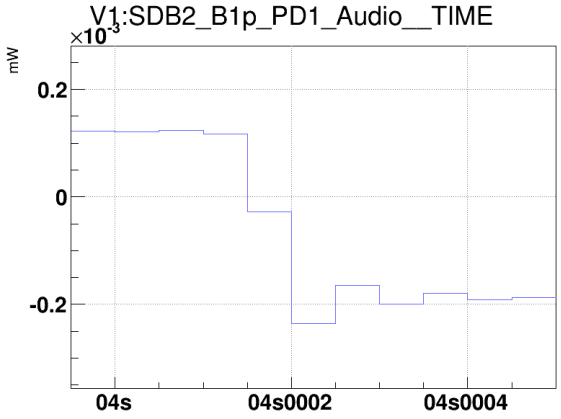

(a) The 20 kHz signals for B1p_PD1, the delay is estimated at 150 $\mu s \leq \tau \leq 200$ μs.

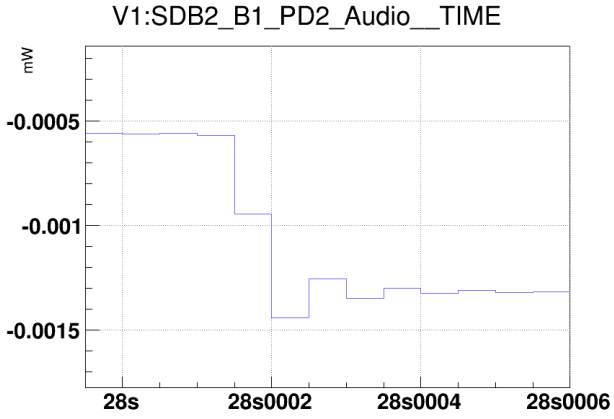

(b) The 20 kHz signals for B1_PD2, the delay is estimated at 150 $\mu s \leq \tau \leq 200$ μs.

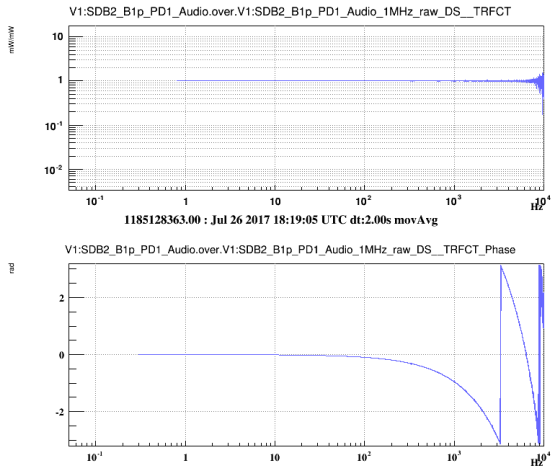

(c) The transfer function between the output signal at 20 kHz and the 1 MHz signal for B1p_PD1.

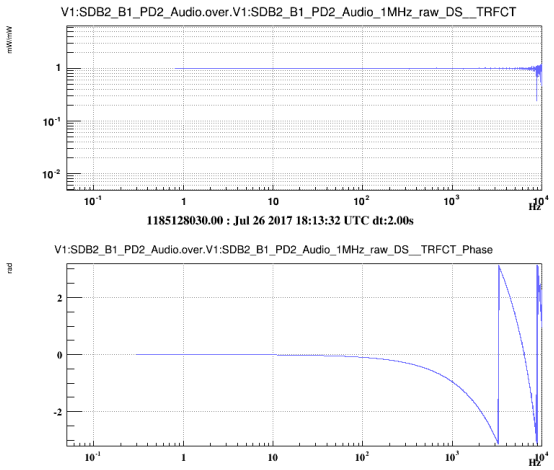

(d) The transfer function between the output signal at 20 kHz and the 1 MHz signal for B1_PD2.

Figure 4: Audio signal at 20 kHz after the Acl process, and transfer function between 20 kHz and 1 MHz.

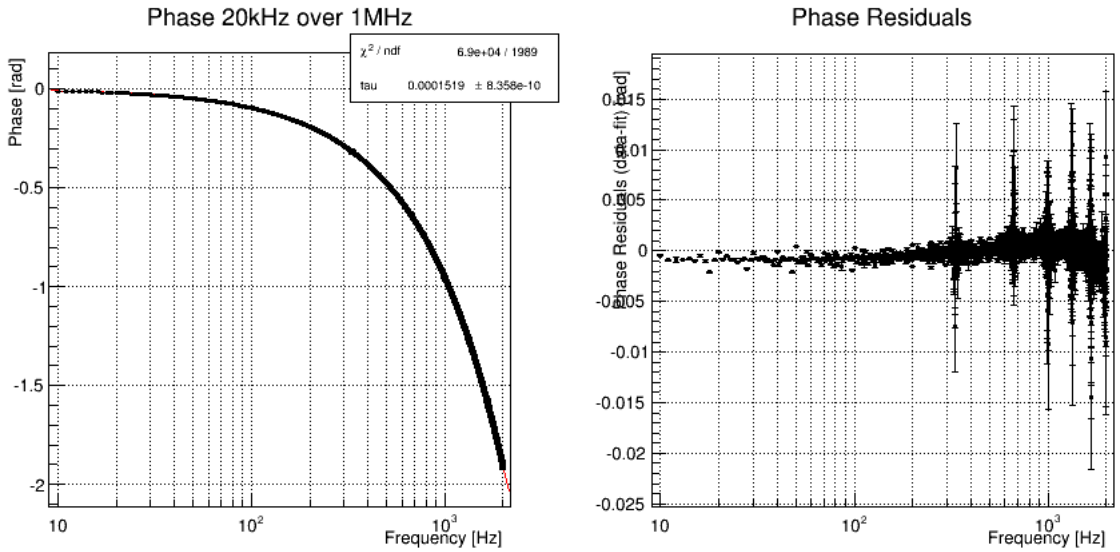

(a) Fit of the phase for B1p_ PD1 between the 20 *kHz channel and the* 1 *MHz channel (left panel) and the residuals (right panel). The delay is fitted at* $\tau_{B1_p} \sim 151.9$ μs *with systematic uncertainty* ≤ 0.2 μs.

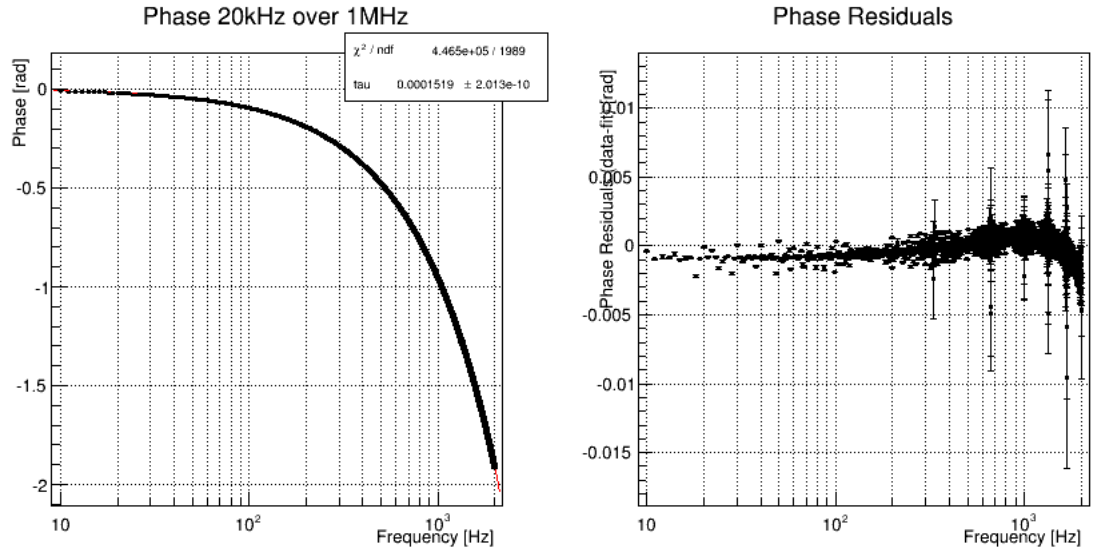

(b) Fit of the phase for B1_ PD2 between the 20 *kHz channel and the* 1 *MHz channel (left panel) and the residuals (right panel). The delay is fitted at* $\tau_{B1} \sim 151.9$ μs *with systematic uncertainty* ≤ 0.2 μs.

Figure 5: Fit and residuals for the phase between 20 kHz and 1 MHz for B1p and B1.

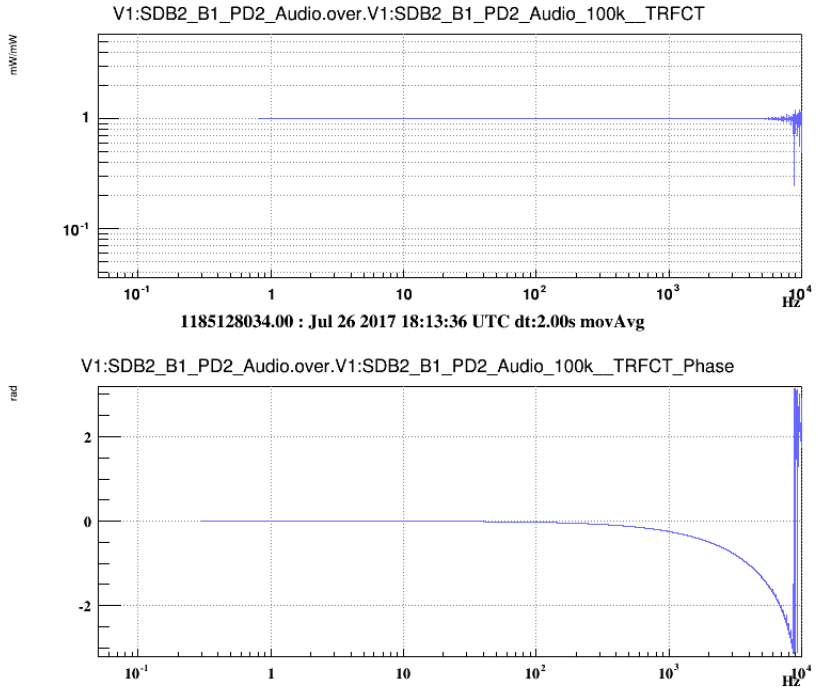

(a) The transfer function between the output signal at 20 *kHz and the* 100 *kHz signal for B1_ PD2.*

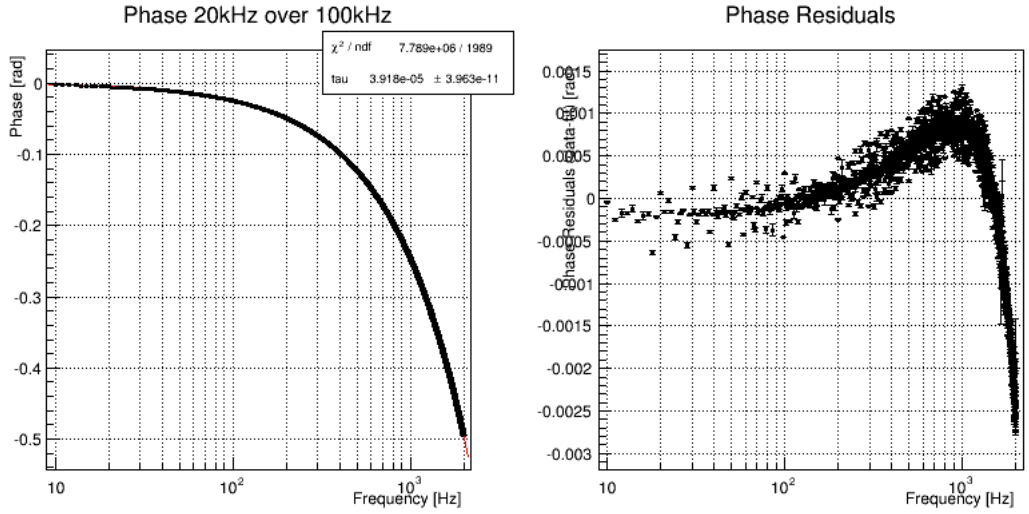

(b) Fit of the phase for SDB2_ B1_ PD2, the delay is $\tau_{20kHz/100kHz} = 39.2\ \mu s$ *with systematic uncertainty* $\sim 0.2\ \mu s$.

Figure 6: Fit and residuals for the phase between 20 kHz and 100 kHz for B1.

1.2.4 Blended 20 kHz channel at the output of the RTPC

The process of reconstruction of the gravitational waves signal h_{rec} uses the Blended 20 kHz channel on B1_PD2 which is a mix of the DC and Audio channels. Figure 7a shows the transfer function between the blended signal at 20 kHz and 1 MHz. We can fit the phase at high frequencies ($\geq$ 500 Hz) with a pure delay and we get $\tau_{blended} \sim 152.4 \pm 0.4$ μs the error coming from systematic uncertainty. The fit and the residuals are shown in Figure 7b. This delay is consistent with the delay we obtain from the Audio channel and this value has been used for the reconstruction of the gravitational waves signal during O2.

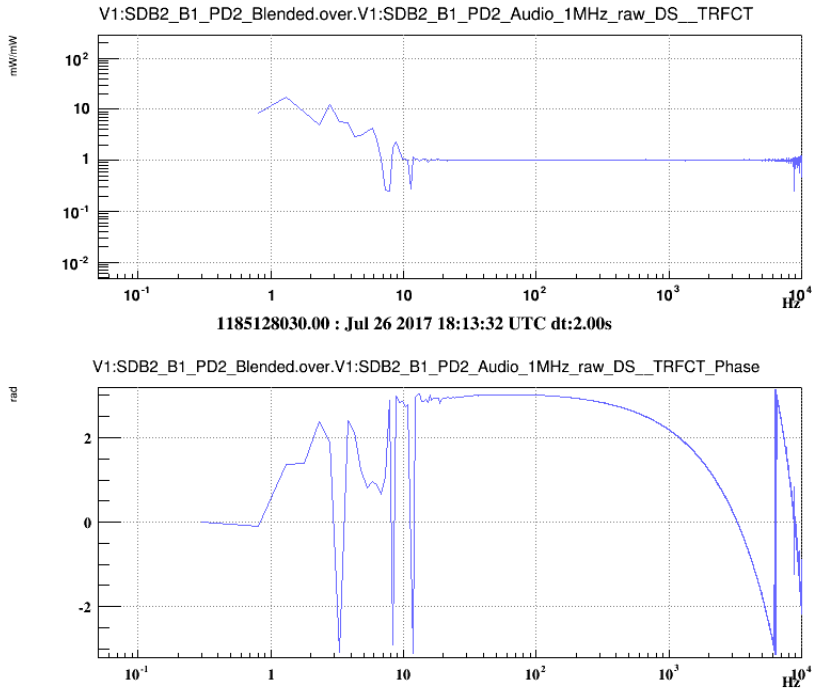

(a) The transfer function between the output signal at 20 *kHz blended and the* 1 *MHz signal for B1_ PD2.*

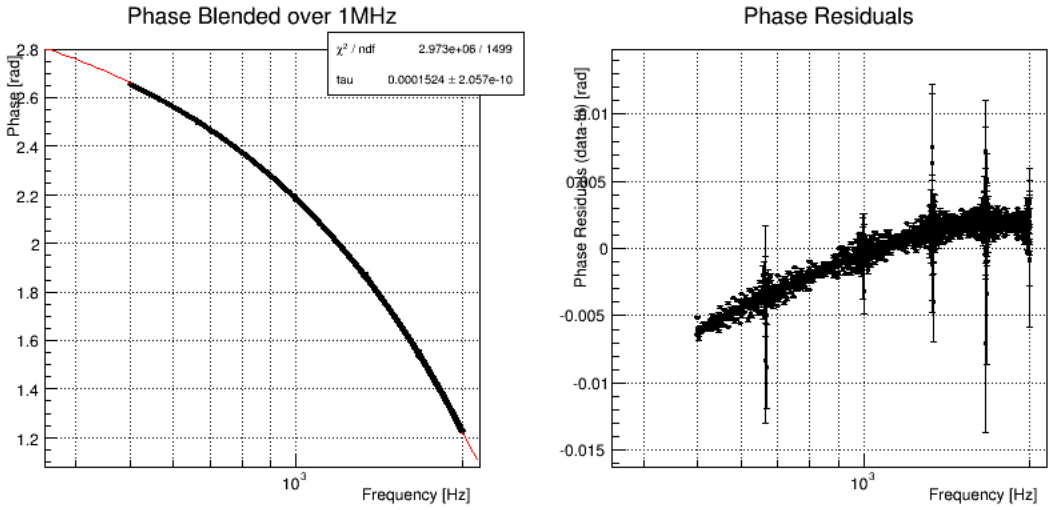

(b) Fit of the phase of the blended signal B1_ PD2 at 20 *kHz over the audio signal at* 1 *MHz from* 500 *Hz to* 2 *kHz. The delay is estimated at* $\tau_{blended} = 152.4$ μs*. The residuals are shown on the right panel. They are within* 5 *mrad which corresponds to* 0.4 μs *at* 2 *kHz.*

Figure 7: Fit and residuals for the phase between blended 20 kHz and 1 MHz for B1.

2 SDB2 B1/B1p timing expectations

2.1 Expectations on the delays considering the different parts of the sensing path

We report here what are the expectations we have on the delays considering the elements forming the sensing path.
For the digital filters, the frequency warping has been taken into account when showing the estimated delays. (Note that the warping was not yet used for the first timing estimation done in note [2])

Analog filter: The analog filter before the ADC is composed of different poles gathered in Table 1 and the theoretical delay up to 2 kHz is $\tau_{ADC} \sim 6.6(\pm 0.001)$ μs as shown in Figure 8.

Filter ADC_2378	f_p (Hz)	Q
pole_0	79577	-
pole_1	74287	0.6348
pole_2	82853	1.562

Table 1: Poles of the filter before the ADC

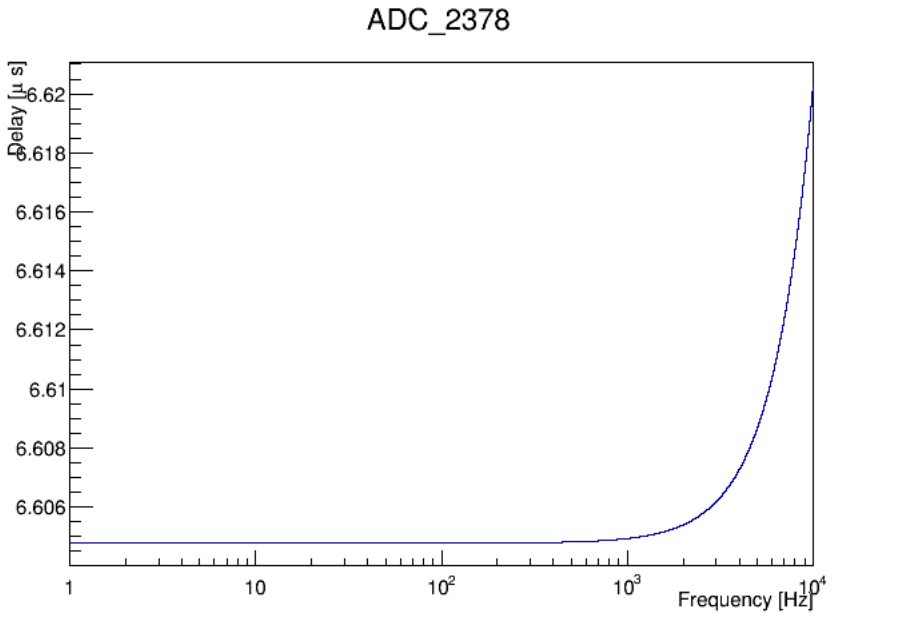

Figure 8: Delay expected for the analog filter. The delay is ~ 6.6 μs.

DSP: Then the DSP is made of a 8^{th} order Butterworth filter with $f_{cut} = 37518$ Hz and a decimation process to go from 1 MHz to 100 kHz. Thus the delay expected for the DSP is composed of a delay of 21.7 μs from the Butterworth filter (Figure 9) and an advance of 9 μs from the decimation which results in a total delay of $\tau_{DSP} \sim 21.7 - 9 = 12.7(\pm 0.02)$ μs.

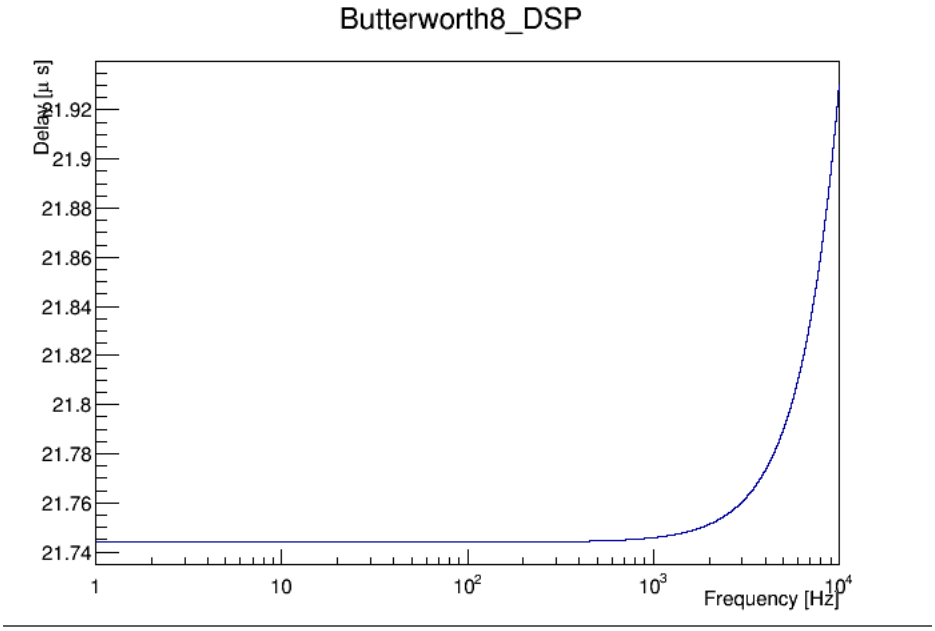

Figure 9: Delay expected for a 8^{th} order Butterworth filter with $f_{cut} = 37518$ Hz. The delay is ~ 21.7 μs.

ACL: The ACL process is composed of a 8^{th} order Butterworth filter with $f_{cut} = 10$ kHz with a few poles and zeros corrections (see Table 2) and a decimation process to go from 100 kHz to 20 kHz. We expect a delay of $\sim 78.9 \pm 0.3$ μs due to the Butterworth filter (Figure 10) and an advance of ~ 40 μs due to the decimation which would result in a total delay $\tau_{Acl} = 78.9 - 40 = 38.9 \pm 0.3$ μs.

Total delay: One cycle of the Acl process induces a delay of $\tau_{cycle} = 100$ μs. Thus, we should expect a total delay of $\tau_{tot} = \tau_{ADC} + \tau_{DSP} + \tau_{cycle} + \tau_{Acl} = 158.2 \pm 0.3$ μs for the output signal at 20 kHz.

Filter ACL	f_p (Hz)	Q
8^{th} Butterworth	10000	-
pole_0	12831.3	2000
pole_1	8747	2000
pole_2	25662.6	2000
pole_3	17494	2000
pole_4	21578.3	2000
zero_0	12831.3	10^6
zero_1	8747	10^6
zero_2	25662.6	10^6
zero_3	17494	10^6
zero_4	21578.3	10^6

Table 2: Butterworth filter and the poles and zeros characteristics.

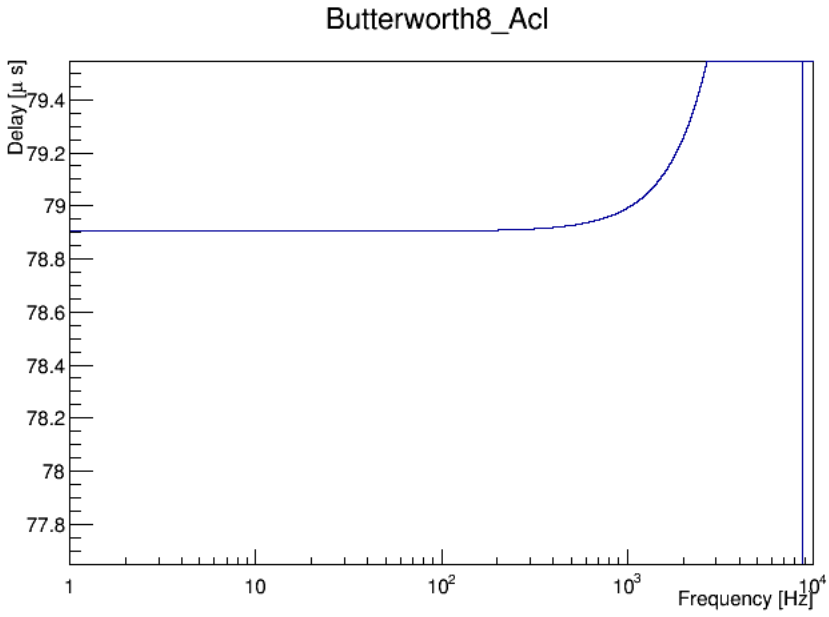

Figure 10: Delay expected for a modified 8^{th} order Butterworth filter with $f_{cut} = 10$ kHz. The delay is ~ 78.9 μs within an uncertainty ≤ 0.3 μs up to 2 kHz.

2.2 Chronogram of the sensing path

Here we present a simple example of a chronogram illustrating how the process in the RTPC works with respect to an input IRIG-B signal.

Channels of the chronogram in Figure 11:

• **GPS:** Split in frames of 100 μs. The red upward arrow is the time t_0 of the GPS occurring every second.

• **DAQ:** cf **GPS**. The GPS time is shifted by 16 μs due to the 3km propagation in the optical fiber.

• **RTPC:** cf **DAQ**. There is a shift of the frames by 16 μs defined by the user due to extra-delay in packets received from DAQ-Boxes. This delay will be invisible at the end of the whole process.

• 100 **kHz sampling:** A 100 kHz sampling synchronized with the DAQ-Box GPS time.

• 1 **MHz sampled signal:** The IRIG-B signal sampled at 1 MHz.

• 100 **kHz sampled signal:** The IRIG-B signal sampled at 100 kHz.

• **Reception RTPC:** The signal after propagation from DAQ-Box to RTPC cycle.

• **Butterworth filter:** The signal after a 8^{th} order Butterworth filtering at 10 kHz.

• **Signal in frames in RTPC:** The signal after decimation after having taken packets of 5 samples starting from the beginning of a frame and putting the last sample of the packet at the beginning of the frame.

• **Signal in frames** (20 **kHz):** The output signal at 20 kHz arranges in frames of 100 μs and corrected of the 16 μs extra-delay for the reception of the packets in the RTPC.

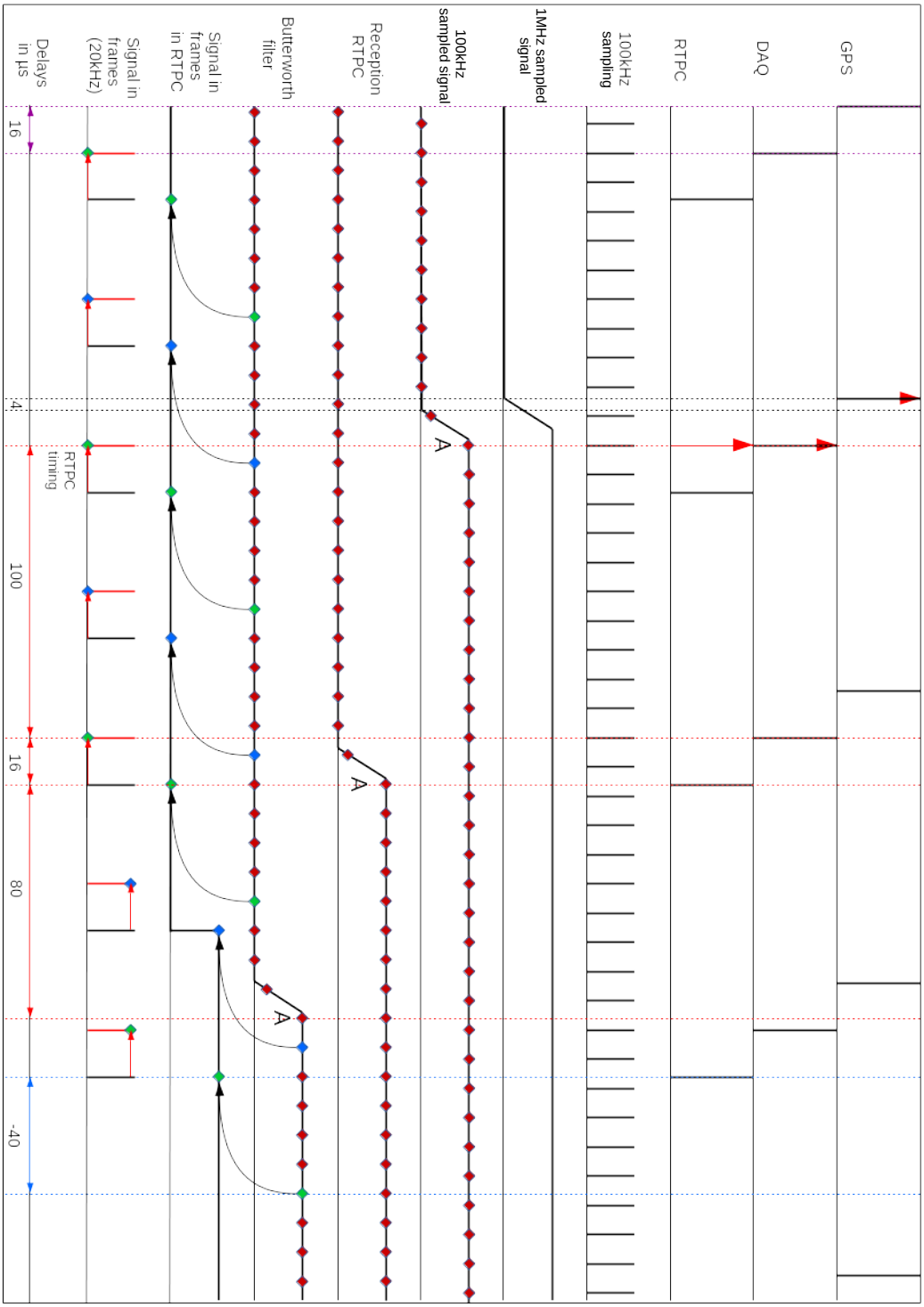

Figure 11: Chronogram of the sensing path

Conclusion

The elements of the sensing path for SDB2_B1/B1p were reported here as well as the measurements done to evaluate the delay induced by this set-up. Table 3 and Table 4 gather all the delays of the sensing path measured and expected.
The measured raw delay is $\tau_{raw} = 155.9 \pm 2$ μs to which we can subtract the 16 μs of the light propagation in the optical fibers and obtain the absolute delay $\tau_{abs} = 155.9 - 16 = 139.9 \pm 3$ μs $\sim 140 \pm 3$ μs. The expected absolute delay is $\tau_{exp} = 158.2 - 16 = 142.2 \pm 1$ μs $\sim 142 \pm 1$ μs. For the run O2, the measured value of 140 μs for the timing of SDB2 has been implemented in the reconstruction of the gravitational waves signal.
The timing of the sensing path is nearly fully understood but there are still 2.6 μs expected that we do not see in the measurements. This difference comes from the analog electronics; the preamplifier with its band-pass filter and the anti-alias ADC filter. Given that we have determined the uncertainty for the timing at ± 20 μs for O2, the 2.6 μs are not an issue for now. Future investigations will be done to better understand this difference between the expected and measured delays.

-		10 Hz $\leq f \leq$ 2 kHz	$\tau_{measured}$ (μs)	$\tau_{expected}$ (μs)
Analog	Audio	-	4 ± 2	6.6
Digital	Audio	100 kHz over 1 MHz	112.8 ± 0.1	112.7
Digital	Audio	20 kHz over 100 kHz	39.2 ± 0.2	38.9 ± 0.3
Digital	Audio	20 kHz over 1 MHz	151.9 ± 0.2	151.6 ± 0.3
Digital	Blended	20 kHz over 1 MHz	152.4 ± 0.4	-
Timing distribution	-	-	[3]	-16 ± 1 μs

Table 3: Delays for every steps in the sensing path.

	$\tau_{measured}$ (μs)	$\tau_{expected}$ (μs)
B1p_PD1_Audio	140 ± 3 μs	$158 - 16 = 142 \pm 1$ μs
B1_PD2_Blended	140 ± 3 μs	$158 - 16 = 142 \pm 1$ μs

Table 4: Total delays for SDB2_B1p and SDB2_B1 channels to be compensated to recover the incident power on the photodiode at absolute GPS time.

References

[1] D. Estevez, V. Germain, F. Marion, B. Mours, L. Rolland, and D. Verkindt. Advanced Virgo calibration for O2: photodiode sensing and mirror and marionette actuator responses. *VIR-0707B-17*, 2017.

[2] D. Estevez, V. Germain, F. Marion, B. Mours, L. Rolland, and D. Verkindt. V1O2Repro1A h(t) reprocessing for Virgo O2 data. *VIR-0706B-17*, 2017.

[3] N. Letendre, A. Masserot, and B. Mours. Virgo+ timing deployment. *VIR-073B-08*, 2009.